JOURNAL OF SOLID STATE CHEMISTRY **134,** 274–281 (1997)
ARTICLE NO. SC977553

Magnetic Properties of the $LaNi_{1-x}W_xO_3$ ($0 \leq x \leq 0.25$) Perovskites

I. Alvarez,*,[1] M. T. Fernández-Díaz,† J. L. Martínez,‡ M. L. Veiga,* and C. Pico*

*Departamento Química Inorgánica I, Facultad de Ciencias Químicas, Universidad Complutense, 28040 Madrid, Spain; †Institut Laue-Langevin, BP 156, F-38042 Grenoble Cedex 9, France; and ‡Instituto de Ciencia de Materiales, CSIC, Cantoblanco, E-28049 Madrid, Spain

Received February 24, 1997; in revised form July 7, 1997; accepted July 15, 1997

Magnetic properties of the $LaNi_{1-x}W_xO_x$ ($0 \leq x \leq 0.25$) mixed oxides have been studied from the temperature and magnetic field (H) dependence of the magnetization (M) and low-temperature neutron diffraction experiments. The variation of M with temperature shows the presence of weak ferromagnetic interactions with Curie temperatures ranging from 200 to 250 K. These interactions become stronger as x increases and this fact has been interpreted in relation to the progressive electronic localization that takes place in this perovskite-like system. The observed ferromagnetic behavior is confirmed by the hysteresis loops obtained in the M vs H curves at different temperatures. The saturation values are however very low in comparison with the expected ones for Ni^{2+} or Ni^{3+}. On the other hand, an extra peak in the neutron diffraction experiments for the $x = 0.20$ phase shows the appearance of an antiferromagnetic ordering, which has been interpreted on the basis of a G-type magnetic mode. Both results can be understood considering antiferromagnetic in character interactions with an important canting of the spin arrangement, giving therefore rise to a weak ferromagnetic component, which has been characterized from magnetization measurements. These results have been summarized in a phase diagram in which the most relevant electronic features of the title system can be visualized.

INTRODUCTION

The metallic properties shown by $LaNiO_3$ are quite uncommon in oxides and, in recent years, considerable attention has been focused on the study of this oxide as it was expected to reveal important aspects to better understand the superconducting behavior presented by some analogous copper-containing compounds (1–5). In this context, some perovskite-like systems derived from $LaNiO_3$, e.g., $RNiO_3$ (R = rare earth), $LaNi_{1-x}M_xO_3$ (M = Cr, Mn, Fe, Co, Cu, Sb), $R_{1-x}M_xNiO_3$ (M = Sr, Th), and $La_{n+1}Ni_nO_{3n+1}$ (6–10), have been extensively studied.

$LaNiO_3$ is known to behave as a metal down to 1.7 K (1, 2) with a large Pauli-type magnetic susceptibility (Stoner enhancement), which has been interpreted in terms of a system with correlated $3d$ electrons in a quarter-filled e_g-type band. In $RNiO_3$ oxides a complex antiferromagnetic ordering has been observed and perovskite systems such as $LaNi_{1-x}M_xO_3$ (M = Cr, Fe, Co) have been reported to show localized or itinerant behavior of the d electrons depending on the composition and/or the temperature, as a consequence of the gradual evolution of a delocalized system such as $LaNiO_3$ to a localized system of the $LaMO_3$ type.

On the other hand, in perovskite systems and related compounds containing mixed-valent nickel ions, such as $La_{n+1}Ni_nO_{3n+1}$ or $La_{3-x}M_xNi_2O_{7-d}$ (M = Ca, Sr, Ba) (11), the magnetic susceptibility data were clearly related to the fact that mixed-valent cations were present: in the first case, the authors suggested a crossover from a fluctuating-valence to a Fermi-liquid-like behavior with increasing n; and, in the second case, the data were interpreted in terms of a partially delocalized system that orders ferromagnetically or antiferromagnetically below 100 K.

The attractive electronic properties displayed by this kind of material have prompted us to prepare and study perovskite-type oxides in which nickel cations are present in mixed-valent state to evaluate the main features involved in their physical properties and their relation with structural aspects. We have previously reported the synthesis, structural characterization, and electrical properties of the title system (12, 13). Metal to insulator (M–I) transitions driven by temperature and composition were observed and related to structural aspects. In this paper, we complete this study and report the magnetic behavior of $LaNi_{1-x}W_xO_3$ ($0 \leq x \leq 0.25$) .

EXPERIMENTAL

The synthesis of $LaNi_{1-x}W_xO_3$ was carried out by the sol–gel method as described elsewhere (13). The dc magnetic measurements were performed with an MPMS-5S magnetometer, which allows the application of a highly homogeneous magnetic field, in the temperature range 1.7–350 K. The neutron diffraction experiments were performed at the D1B and D2B powder diffractometers of the Institut

[1] To whom correspondence should be addressed.

0022-4596/97 $25.00

Laue-Langevin (Grenoble, France). The wavelengths used were 2.524 and 1.5945 Å, respectively. For the low-temperature measurements, the sample was placed in a helium cryostat, using a vanadium can. The temperature stability was better than ca. $\pm$ 0.1 K. The diffractometer is equipped with a position-sensitive detector (PSD) spanning an angular range of 80° (2θ) for D1B and a bank of single detectors spanning an angular range of 160° (2θ) for D2B. Neutron diffraction data were analyzed with the Rietveld method by means of the Fullprof program (14).

RESULTS AND DISCUSSION

X-ray, electron, and neutron diffraction data showed that the title perovskites are orthorhombic (with the exception of the $x = 0$ member, that is, $LaNiO_3$, which crystallizes in the trigonal space group $R3c$, as previously reported (1–3) with space group *Pbnm* and cell parameters that can be related to the ideal cubic ($a_c \sim 3.9$ Å) one as follows: $a \sim b \sim \sqrt{2}a_c$; $c \sim 2a_c$. In this structure, no ordering of the three kinds of cations in the B sublattice (W^{6+}, Ni^{3+}, Ni^{2+}) is observed, but they are randomly distributed in the octahedral sites of the perovskite structure. Crystallographic results from X-ray diffraction data were reported earlier (13) for the title compounds. To confirm these structural results and to study the magnetic structure shown by the $LaNi_{1-x}W_xO_3$ mixed oxides, we have studied the title oxides from powder neutron diffraction experiments and we have analyzed them by means of the Rietveld method. Figure 1 shows, for the $x = 0.20$ sample as an example, the observed and calculated powder neutron diffraction (D2B) profiles, the difference between them, and the allowed reflections at room temperature. The best fit was obtained considering a certain amount (3.5%, as obtained from Rietveld refinement) of

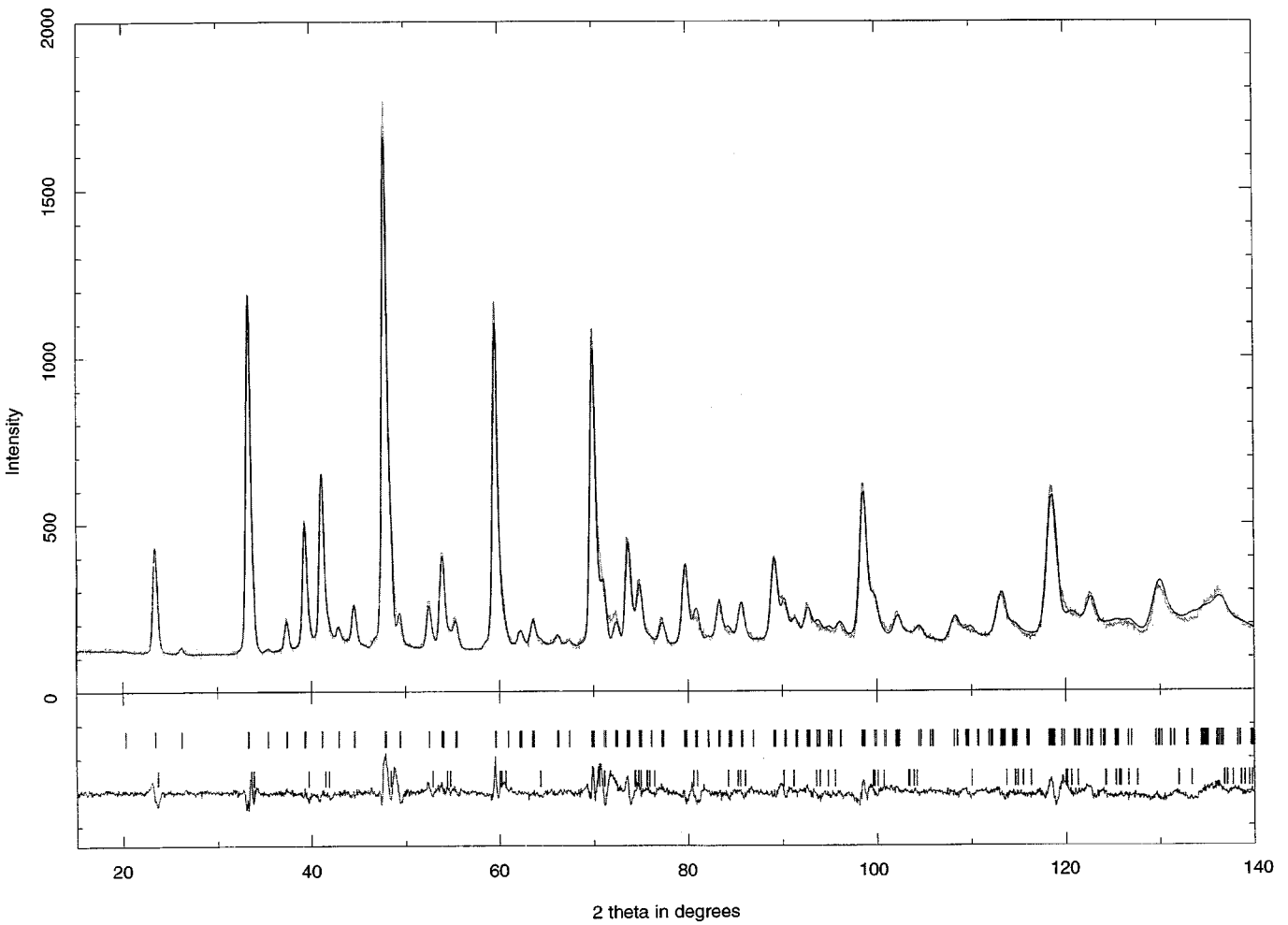

FIG. 1. Observed (dotted line), calculated (solid line), and difference neutron diffraction profiles (D2B) for $LaNi_{0.80}W_{0.20}O_3$. Vertical bars correspond to the allowed reflections and the second row to $LaNiO_3$ (see text).

TABLE 1
Crystal Data for $LaNi_{0.80}W_{0.20}O_3$ from Neutron Diffraction Measurements at Room Temperature[a]

Atom	Position	x	y	z	β(Å^2)
La	4*c*	0.011(1)	0.037(5)	0.25	1.72(4)
Ni/W	4*b*	0.5	0	0	0.44(2)
O(1)	8*d*	0.2893(8)	0.2844(8)	0.0398(6)	1.33(3)
O(2)	4*c*	− 0.017(1)	0.496(1)	0.25	0.999(4)

[a] $a = 5.5558(5)$ Å, $b = 5.5746(5)$ Å, $c = 7.8485(7)$ Å; Space group *Pbnm*; $R_p = 4.28$, $R_{wp} = 5.58$, $R_F = 2.86$, $\chi^2 = 3.53$, $R_B = 4.44$.

a $LaNiO_3$ phase and it was considered as a second phase in the refinement. The results obtained from this refinement are gathered in Table 1.

Figure 2a shows the variation of magnetic susceptibility with temperature ranging between 1.7 and 300 K for a magnetic field of 5000 Oe. To better visualize the shape of the curves, in Fig. 2b these graphs are shown in a selected temperature scale. In all cases an almost temperature-independent behavior is observed above ~ 250 K, consistent with a Pauli paramagnetism with a $\chi_{RT} \sim 10^{-4}$ emu·mol^{-1} (where RT designates room temperature), and this can be related to the existence of an important eletronic delocalization above this temperature. This enhanced χ value indicates a relatively strong correlation among the 3*d* electrons in a narrow band as has been reported earlier for the $x = 0$ phase (5) and other similar compouds such as $BaNbO_3$ (15). Below ~ 250 K, a marked enhancement of magnetization values with decreasing temperature is observed, which, in

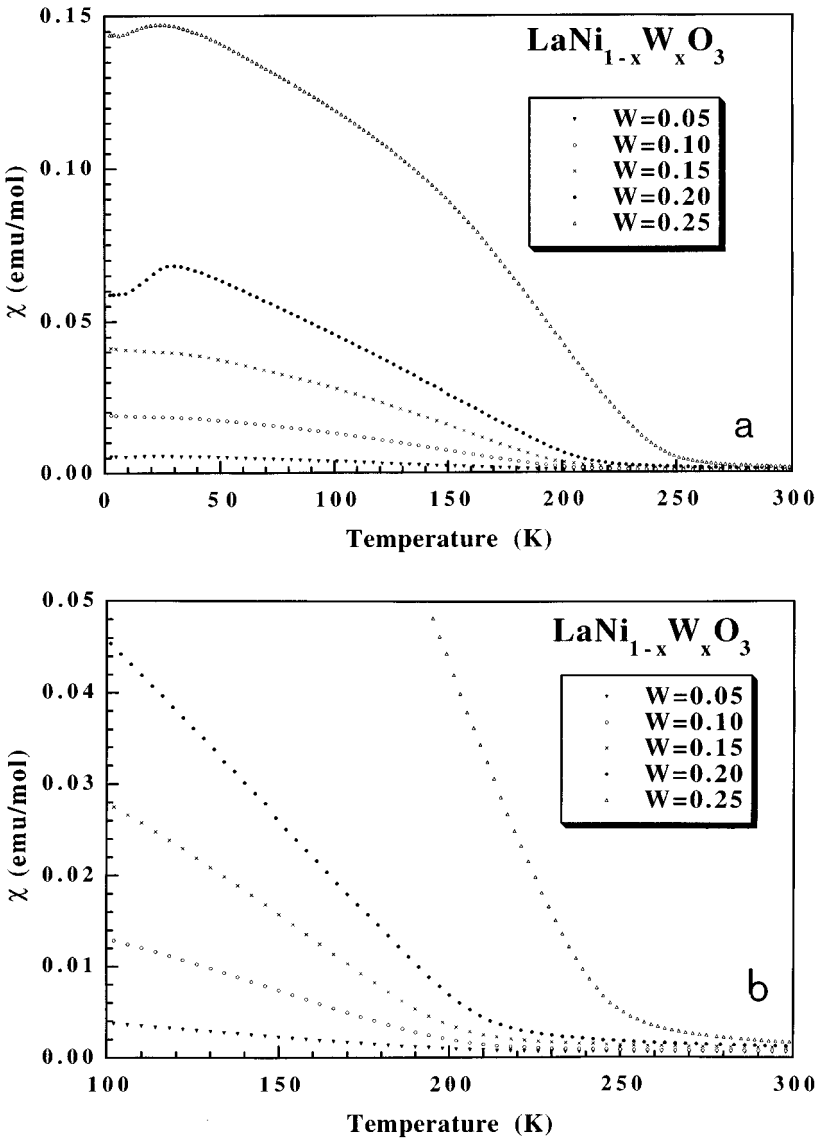

FIG. 2. Variation of the magnetic susceptibility at 5000 Oe with the temperature (a) between 1.7 and 300 K and (b) between 100 and 300 K for $LaNi_{1-x}W_xO_3$ ($0 \le x \le 0.25$).

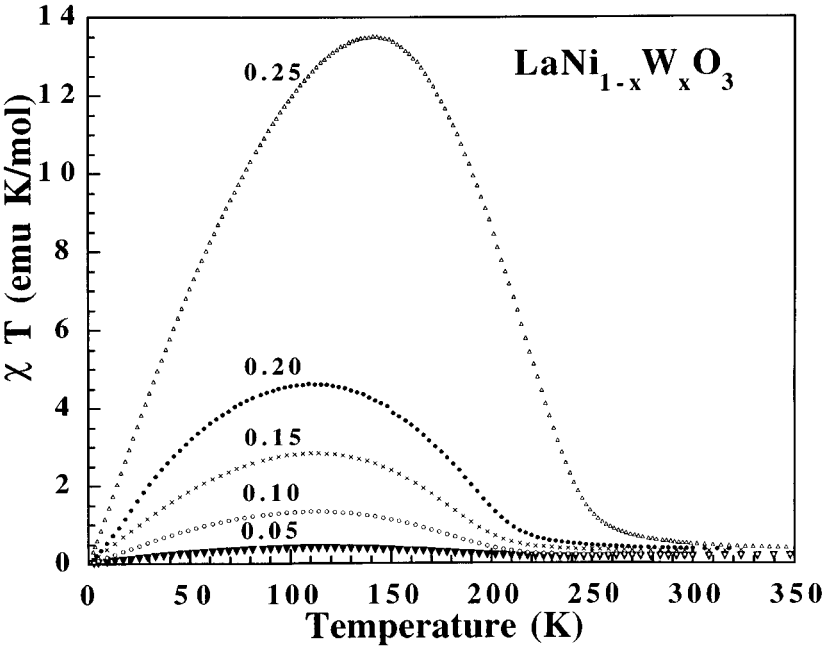

FIG. 3. Variation of χT vs T at 5000 Oe for $LaNi_{1-x}W_xO_3$ ($0 \leq x \leq 0.25$).

principle, can be associated with ferromagnetic interactions in all the materials, with Curie temperatures of ca. 215 K for $0.05 \leq x \leq 0.20$ and 255 K for the $x = 0.25$, respectively. This magnetization response becomes stronger as x is increased and this confirms that an electronic localization stabilizes in this system as x values become greater (i.e., as the amount of Ni^{2+} is increased). This is in good agreement with the electrical resistivity measurements previously reported (13), as it was stated that a M–I transition takes place as a function of x, being semimetallic for $x \leq 0.2$ and semiconducting for $x = 0.25$. In Fig. 3 the variation of χT vs T at 5000 Oe is shown. It can be observed that there is a transition from a paramagnetic phase to a weak ferromagnetic phase below ~ 250 K. It is worth noting two important aspects from the graph:

(a) The fit of the paramagnetic region data to a Curie–Weiss law gives magnetic moments much smaller than the expected ones considering only the relative amounts of Ni^{2+}/Ni^{3+}. In Table 2 the observed and calculated magnetic moments above 250 K are gathered. These results are probably due to the small temperature range available (250–350 K); that is, the transition temperature has not been widely overcome.

(b) On the other hand, in Fig. 3 it can be observed that below ~ 150 K, the magnetic moment values sharply decrease. This fact could indicate the complex nature of the magnetic interactions, which could be antiferromagnetic in character or, at least, there could exist a competition between antiferromagnetic and ferromagnetic interactions in these systems. Below 50 K, the magnetization varies anomalously with temperature in a similar way to that reported previously for some nickel mixed-valence systems in which the magnetic behavior was related to the fluctuating valence of Ni cations (8, 11).

To confirm the observed weak ferromagnetism, the variation of the magnetization with the magnetic field at different temperatures and for all the samples has been measured. In Figs. 4a and 4b, the corresponding variations at 5 K for all the series members are shown. As can be observed, the materials could be classified as hard ferromagnets as they present relatively high values of remanent magnetization, with coercive fields of ca. 1 kOe at 20 K. The hysteresis loops at different temperatures for the least and most doped compounds (with $x = 0.05$ and $x = 0.25$) are shown in

TABLE 2
Observed (Considering a Curie–Weiss Law) and Calculated Magnetic Moments above 250 K

x	% Ni^{3+}	$\mu_o{}^a$ (μ_B)	$\mu_c{}^b$ (μ_B)	$\Delta(\mu_c - \mu_o)$ (μ_B)
0.05	80	2.41	3.63	1.22
0.10	60	1.70	3.38	1.68
0.15	40	1.34	3.10	1.76
0.20	20	1.23	2.79	1.56
0.25	0	1.09	2.45	1.36

[a] Magnetic moment obtained from the Curie–Weiss law fit.

[b] Magnetic moment calculated from the Curie constant obtained as follows: $C = zC_{Ni^{3+}} + (1 - x - z)\,C_{Ni^{2+}}$, where z is the Ni^{3+} percentage per Ni^{3+} ion in the B sites of perovskite.

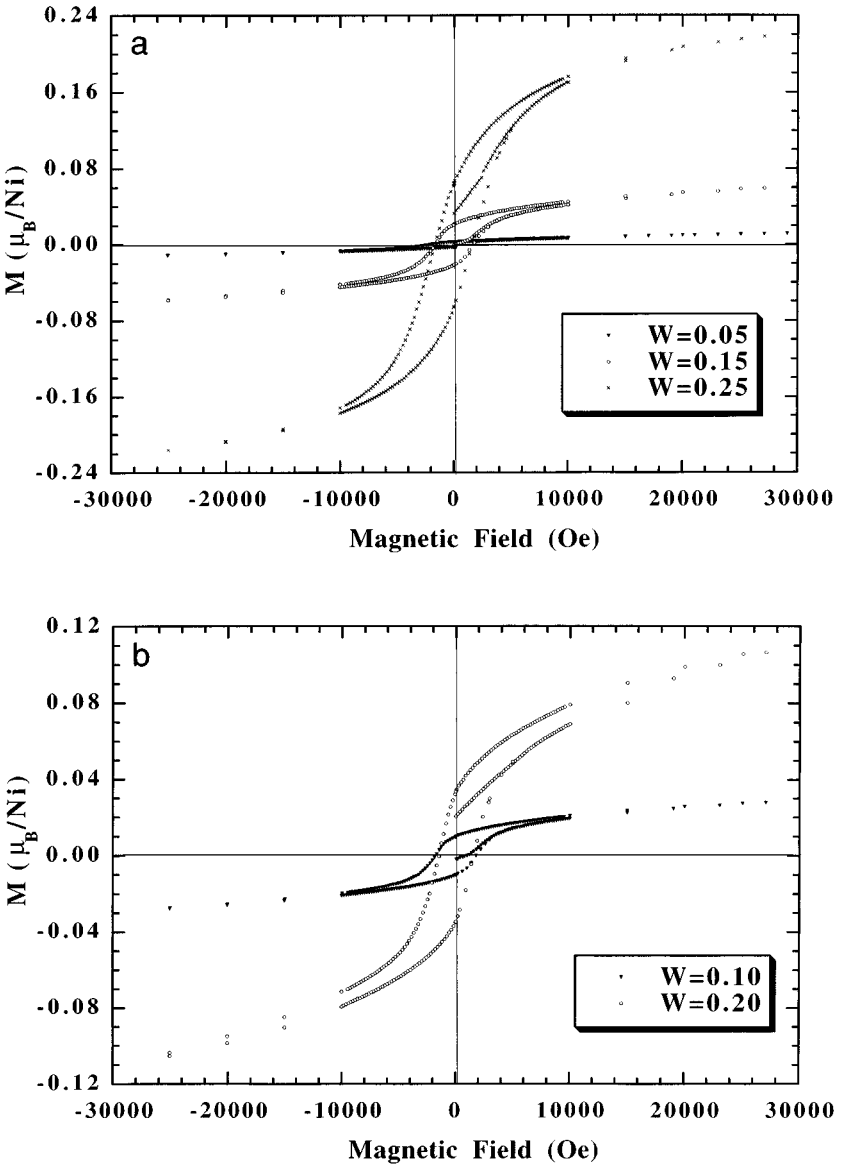

FIG. 4. Variation of magnetization with the magnetic field at 5 K (a) for the $x = 0.05, 0.15$, and 0.25 phases and (b) for the $x = 0.10$ and 0.20 compounds (two graphs have been used for clarity).

Figs. 5 and 6, respectively. From these graphs it can be deduced that ferromagnetic order disappears at 215 K for the $x = 0.05$ phase and at 255 K for the $x = 0.25$ compound. With similar measurements for the rest of the materials, the Curie temperatures mentioned earlier could be estimated. In Tables 3 and 4, the most representative magnetic parameters, obtained at different temperatures for the $x = 0.05$ and 0.25 phases, are gathered. An important aspect is that the saturation moments obtained in these isothermal magnetization curves are very low ($< 0.20\ \mu_B$/Ni atom), which indicates a low correlated ferromagnetic moment. This is particularly clear in the case of $LaNi_{0.75}W_{0.25}O_3$, where the saturation (spin only) high-spin Ni^{2+} (d^8) is close to 2 μ_B/Ni atom. For the mixed-valence system ($x < 0.25$), the moments are also very weak but in these cases the long-range correlations could be disturbed by the random mixture of Ni^{2+} and Ni^{3+}.

To characterize the magnetic behavior of the title materials, some low-temperature neutron diffraction measurements have been made. We have not observed any relevant changes in the intensity of the Bragg peaks, which could be related to the weak ferromagnetic ordering observed in the magnetization measurements. This is probably due to the small value of the ferromagnetic component (in general $< 0.2\ \mu_B$) as estimated for these phases from magnetization measurements. We have however noticed the appearance of

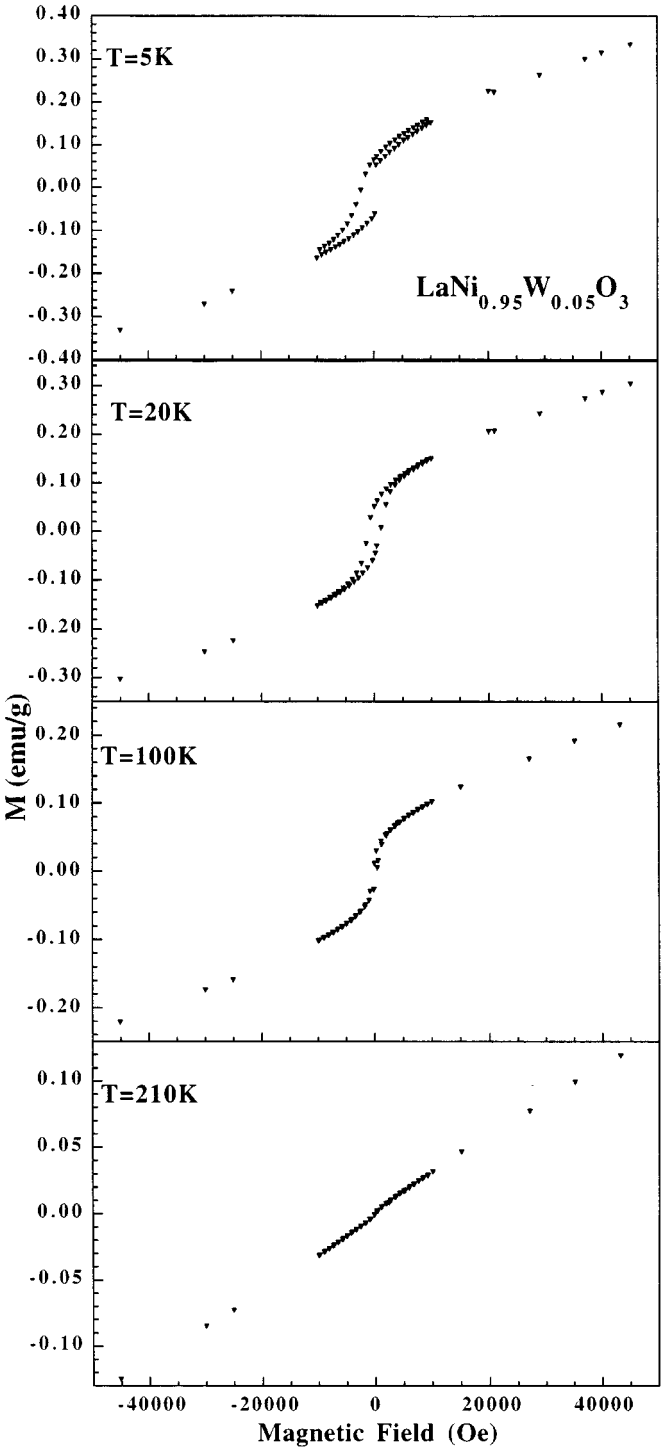

FIG. 5. Variation of magnetization with the magnetic field at 5, 20, 100, and 220 K for the $x = 0.05$ compound ($LaNi_{0.95}W_{0.05}O_3$).

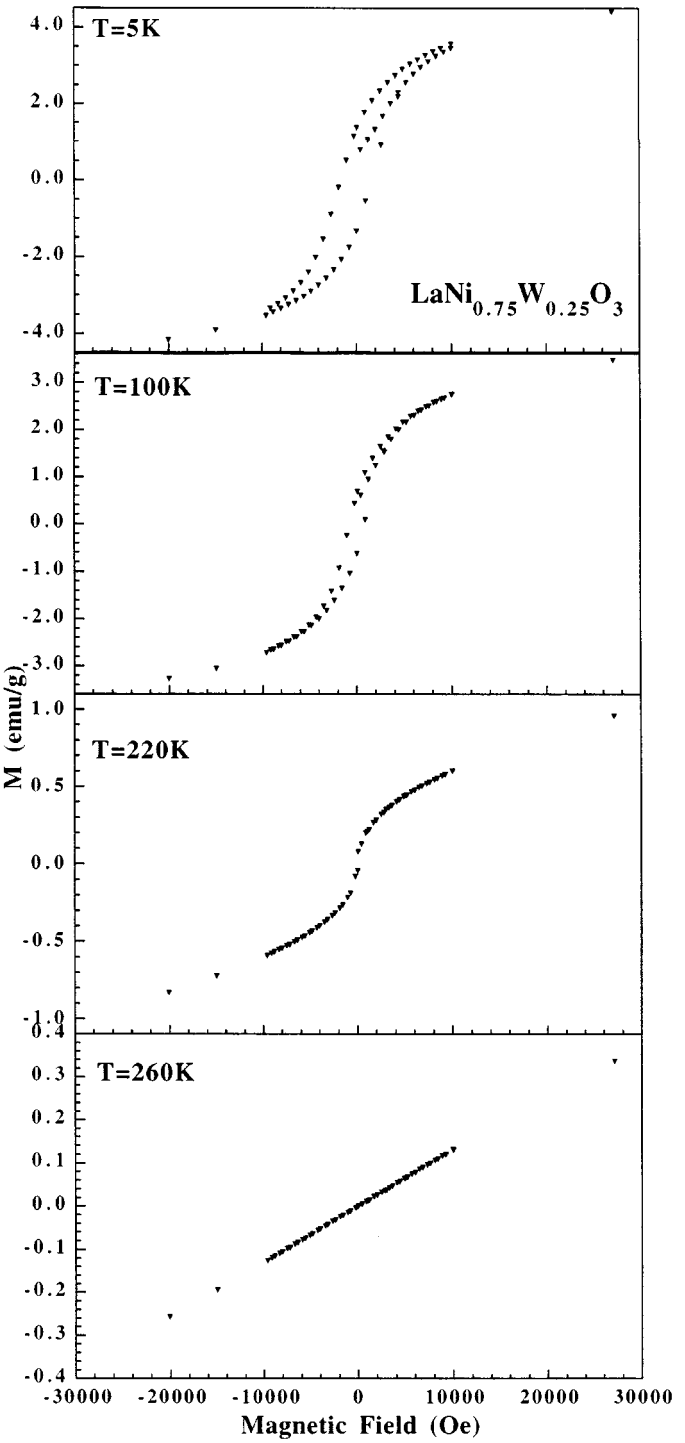

FIG. 6. Variation of magnetization with the magnetic field at 5, 100, 220, and 260 K for the $x = 0.25$ compound ($LaNi_{0.75}W_{0.25}O_3$).

an extra peak in the sample with $x = 0.20$ at low angle ($2\theta \sim 32^\circ$ for $\lambda = 2.52$ Å; $hkl = 101$). The magnetic evolution of this peak (Fig. 7) shows its magnetic origin and its intensity onset take place at the Curie temperature. This fact indicates that the antiferromagnetic and ferromagnetic ordering takes place simultaneously. The observed behavior could therefore be explained considering an antiferromagnetic spin arrangement with a ferromagnetic canting.

TABLE 3

Magnetic Parameters for $LaNi_{0.95}W_{0.05}O_3$: Saturation Magnetization (M_S), Remanent Magnetization (M_R), and Coercive Field (H_C)

T (K)	M_S (μ_B/Ni)	M_R (μ_B/Ni)	H_C (Oe)
5	0.0052	0.0029	2100
20	0.0048	0.0022	1100
100	0.0030	0.0009	250
200	0.0003	0.00009	40

Similar results have previously been interpreted in relation to the existence of noncollinear spin structures (16).

The refinement of the low-temperature diffraction data gives a G-type antiferromagnetic ordering which allows an F-type component. The two possibilities are a G_xF_z mode or a G_zF_x mode. There is not enough information to distinguish

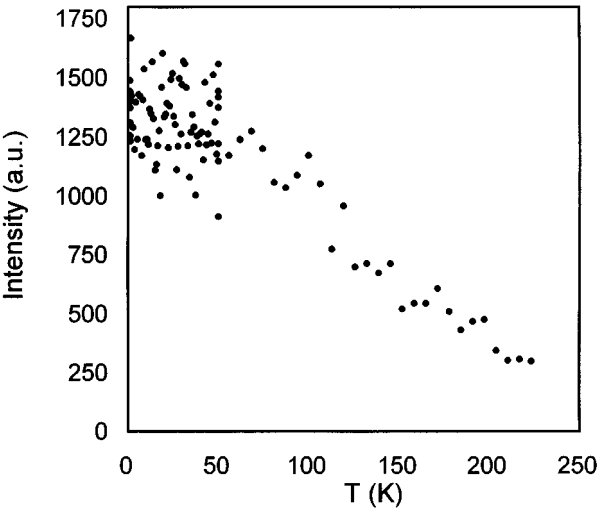

FIG. 7. Temperature dependence of the observed magnetic peak ($2\theta \sim 32°$, for $\lambda = 2.52$ Å, $hkl = 101$) for $LaNi_{0.80}W_{0.20}O_3$.

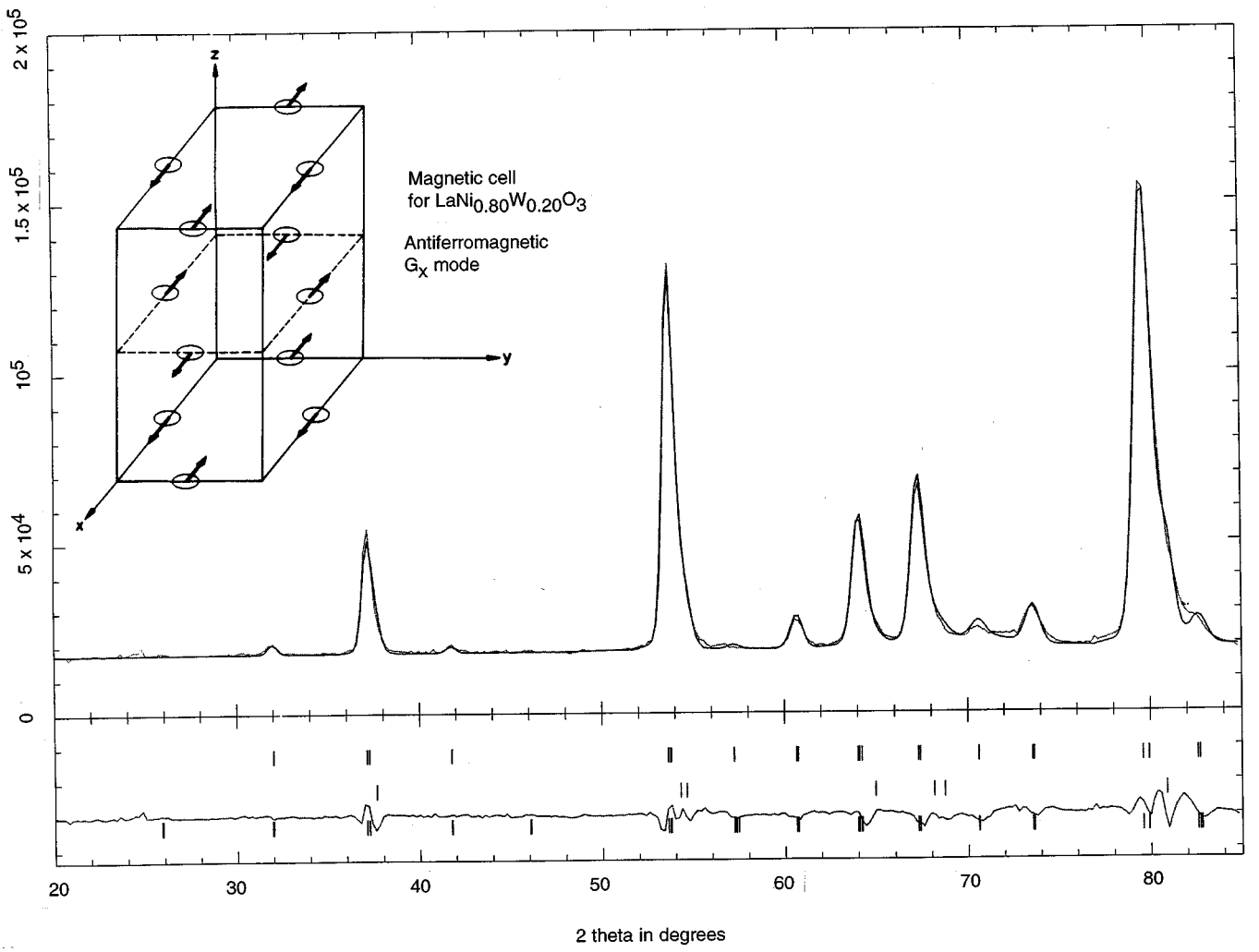

FIG. 8. Observed (dotted line), calculated (solid line), and difference neutron diffraction profiles (D1B) for $LaNi_{0.80}W_{0.20}O_3$. Vertical bars correspond to the allowed reflections. The second row corresponds to $LaNiO_3$ (see text) and the third row to the magnetic structure.

TABLE 4

Magnetic Parameters for $LaNi_{0.75}W_{0.25}O_3$: Saturation Magnetization (M_S), Remanent Magnetization (M_R), and Coercive Field (H_C)

T(K)	M_S (μ_B/Ni)	M_R (μ_B/Ni)	H_C (Oe)
5	0.171	0.0720	2000
100	0.129	0.0397	1000
200	0.043	0.0115	80
220	0.021	0.0059	110
240	0.008	0.0010	20

between both orientations of the magnetic moments. Figure 8 shows the observed, calculated, and difference neutron diffraction profiles at 2 K for the $x = 0.20$ sample (the R factor for the magnetic phase was 18.6). In the inset of this figure, the magnetic cell, considering a G_x mode, is represented. The antiferromagnetic ordered moment at 2 K is 1.4(2) μ_B per Ni ion for the $x = 0.20$ compound. This value is clearly smaller than that expected for ordered Ni^{2+} or Ni^{3+} cations ($1.7 < \mu\ (\mu_B) < 2.8$), indicating an important delocalization in the system. This fact is in good agreement with the resistivity results reported earlier for the title system (13), which evidenced an intermediate behavior between a metal and an insulator for this compound.

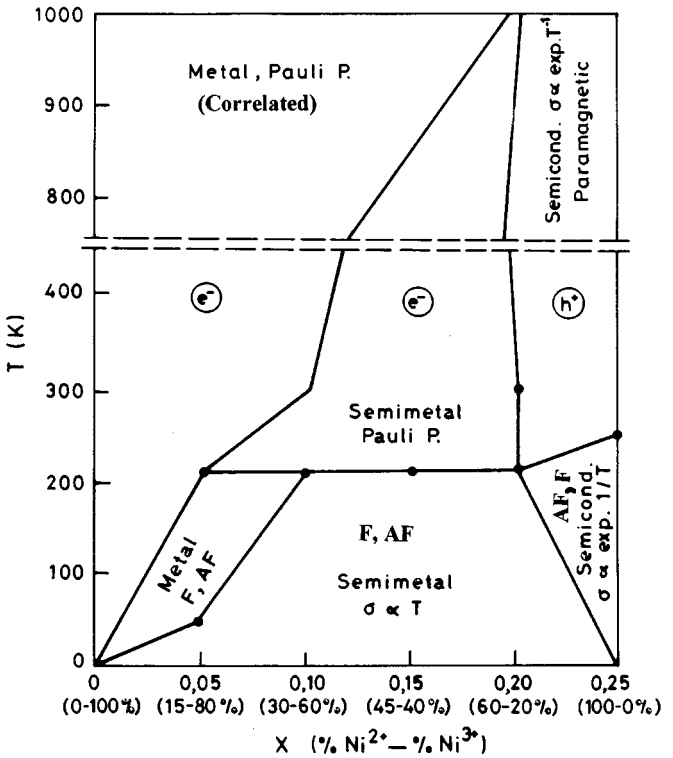

FIG. 9. Temperature–composition phase diagram for the $LaNi_{1-x}W_xO_3$ system. % Ni^{n+} = (Ni^{n+} cations)/(B-sublattice cations) × 100; F = weak ferromagnetic interactions; AF = antiferromagnetic interactions; Pauli P = Pauli paramagnetism; h^+ = p-type conduction; e^N = n-type conduction.

The electronic behavior of $LaNi_{1-x}W_xO_3$ ($0 \le x \le 0.25$) is summarized in the temperature–composition phase diagram shown in Fig. 9. All the electrical and magnetic observed features have been included. As can be observed, two M–I transitions take place in this system:

(a) From left to right in the diagram, corresponding to the increase of Ni^{2+} concentration, the material's behavior changes from that of a metal to that of an insulator; that is, a progressive electronic localization takes place as x increases. This effect includes the progressive stabilization of more important localized magnetic ordering with more noticeable magnetization responses.

(b) From bottom to top, the electronic behavior of these compounds changes also from metallic to insulator. In this sense, increasing temperature has the same effect in electronic properties as decreasing x. As temperature increases, a progressive tendency to electronic delocalization is observed, related to structural aspects (probably driven by entropic factors, as pointed out elsewhere (17)), which is associated with the progressive loss of the magnetic ordering.

ACKNOWLEDGMENTS

We thank the DGICYT (Project PB 94-0214, Spain) and the CICYT (Project MAT 97-0326, Spain) for financial support.

REFERENCES

1. J. B. Goodenough, N. F. Mott, M. Pouchard, G. Demazeau, and P. Hagenmuller, *Mater. Res. Bull.* **8,** 647 (1973).
2. J. P. Kemp and P. A. Cox, *Solid State Commun.* **75,** 731 (1990).
3. J. B. Torrance, P. Lacorre, C. Asaveroengchai, and R. M. Metzger, *J. Solid State Chem.* **90,** 168 (1991).
4. K. P. Rajeev, G. V. Shivashankar, and A. K. Raychaudhuri, *Solid State Commun.* **79,** 591 (1991).
5. K. Sreedhar, J. M. Honig, M. Darwin, M. McElfresh, P. M. Shand, J. Xu, B. C. Crooker, and J. Spalek, *Phys. Rev. B* **46,** 6382 (1992).
6. J. A. Alonso, M. J. Martínez-Lope, and M. A. Hidalgo, *J. Solid State Chem.* **116,** 146 (1995).
7. G. V. Bazuev, V. N. Kasilnikov, N. A. Kirsanov, and N. V. Lukin, *Physica C* **230,** 1631 (1994).
8. K. Sreedhar, and J. M. Honig, *J. Solid State Chem.* **111,** 147 (1994).
9. I. Alvarez, M. L. Veiga, and C. Pico, *J. Less-Common Met.*, in press.
10. P. Lacorre, J. B. Torrance, J. Pannetier, A. I. Nazzal, P. W. Wang, and T. C. Huang, *J. Solid State Chem.* **91,** 225 (1991).
11. Z. Zhang, and M. Greenblatt, *J. Solid State Chem.* **111,** 141 (1994).
12. I. Alvarez, M. L. Veiga, and C. Pico, *J. Mater. Chem.* **5,** 1049 (1995).
13. I. Alvarez, J. L. Martínez, M. L. Veiga, and C. Pico, *J. Solid State Chem.* **125,** 47 (1996).
14. J. Rodríguez-Carvajal, "Fullprof: A program for Rietveld refinement and pattern matching analysis". "Abstracts of Satellite Meeting on Powder Diffraction, XVth Congress of the International Union of Crystallography," Toulouse, 1990, p 127. [revised version, 1994]
15. M. T. Casais, J. A. Alonso, I. Rasines, and M. A. Hidalgo, *Mater. Res. Bull.* **30,** 201 (1995).
16. A. Ahmad, *J. Mater. Sci.* **27,** 4120 (1992).
17. J. B. Torrance, P. Lacorre, A. I. Nazzal, E. J. Ansaldo, and Ch. Niedermayer, *Phys. Rev. B* **45,** 8209 (1992).